SF2A 2011
G. Alecian, K. Belkacem, R. Samadi and D. Valls-Gabaud (eds)

AUTOMATED DETECTION AND TRACKING OF SOLAR AND HELIOSPHERIC FEATURES IN THE FRAME OF THE EUROPEAN PROJECT HELIO

X. Bonnin[1], J. Aboudarham[1], N. Fuller[1], C. Renie[1], D. Perez-Suarez[2], P. Gallagher[2], P. Higgins[2], L. Krista[2], A. Csillaghy[3] and R. Bentley[4]

Abstract. In the frame of the European project HELIO, the Observatoire de Paris-Meudon is in charge of the Heliophysics Feature Catalogue (HFC), a service which provides access to existing solar and heliospheric feature data. In order to create a catalogue as exhaustive as possible, recognition codes are developed to automatically detect and track features. At the time, HFC contains data of filaments, active regions, coronal holes, sunspots and type III radio bursts for a full solar cycle. The insertion of prominences and type II radio bursts should be done in the short term. We present here an overview of some of the algorithms used to populate HFC. The development of such fast and robust techniques also addresses the needs of the Space Weather community in terms of near real-time monitoring capabilities.

Keywords: heliophysics, solar system, virtual observatory, automatic detection, image processing, monitoring, space weather, HELIO, HFC

1 Introduction

The Heliophysics Integrated Observatory, HELIO, is a FP7 European virtual observatory project devoted to solar physics and heliophysics (`http://www.helio-vo.eu/`). At the end of its development, in may 2012, it will supplies dedicated tools as well as coordinate access to large amounts of resources available in the different fields covered by heliophysics. To achieve its goals, it is currently deploying a distributed network of services that will help users to efficiently analyse, handle, reach and/or mine relevant data.
One of theses services, the Heliophysics Feature Catalogue (HFC), provides access to existing solar and heliospheric features data. Like most of HELIO components, HFC will be accessible through various interfaces such as HELIO Front End*, dedicated workflows, application programming interfaces (API), Solar SoftWare (SSW), or using its own graphical user interface (which can be reached at `http://voparis-helio.obspm.fr/hfc-gui/index.php`). In order to offer the most exhaustive feature database, HFC has been regularly updated with new data, which are extracted from observations by automated recognition codes. These codes uses image processing methods developed in the frame of the project (mainly by LESIA in France and TCD in Irland), or provided by the community itself.
We present here a brief overview of some of the algorithms currently available in HELIO and concerning: active regions and coronal holes observed on SOHO/MDI and SOHO/EIT respectively, solar filament detected and tracked on Halpha observations of the Meudon spectroheliograms, but also type III solar radio bursts reported on Wind/Waves dynamical spectra. First section is devoted to Solar feature detection and tracking, and Section 2 to heliophysics feature recognition. Section 3 will conclude presenting the future works.

[1] Observatoire de Paris, section de Meudon, LESIA, UMR 8109 CNRS, 92195 Meudon CEDEX, France
[2] Trinity College Dublin, College Green, Dublin 2, Ireland.
[3] Institute of 4D Technologies, FHNW, Steinackerstrass 5, CH-5210 Windisch, Switzerland
[4] MSSL, University College London, Hombury St. Mary, Dorking, Surrey RH5 6NT, U.K.
*available at `http://helio.i4ds.technik.fhnw.ch/Helio/prototype/explorer`.

2 Recognition of Solar features

2.1 Photospheric Active Regions

The *Solar Monitor Active Region Tracking* (SMART) algorithm (Higgins et al. 2011) allows detection and tracking of active regions (ARs) on solar magnetograms. It has been successfully applied on SOHO/MDI data (Scherrer et al. 1995), and is currently used in the frame of HELIO to provide magnetic and location information to HFC, for a period spanning the entire solar cycle 23. To extract ARs from an image, the SMART method is based on three successive steps: (i) a *segmentation* process (including cleaning process and quiet sun background subtraction) that produces a binary mask of features using threshold technique. (ii) A *characterization* process, which extracts magnetic properties from previous feature masks such as statistical moments of the magnetic field and the minimum and maximum magnetic field values. (iii) a *classification* step that permits to discriminate between various feature types.
Figure 1 shows result of ARs detection by SMART on a SOHO/MDI magnetogram. This image of the Sun, observed on June 10, 2001 at 00:00:01 (UTC) and produced as an output by HFC, presents several ARs localizable thanks to their white line contours. The ARs gravity centers are represented by white dots, and the corresponding NOAA region numbers are given in brackets.

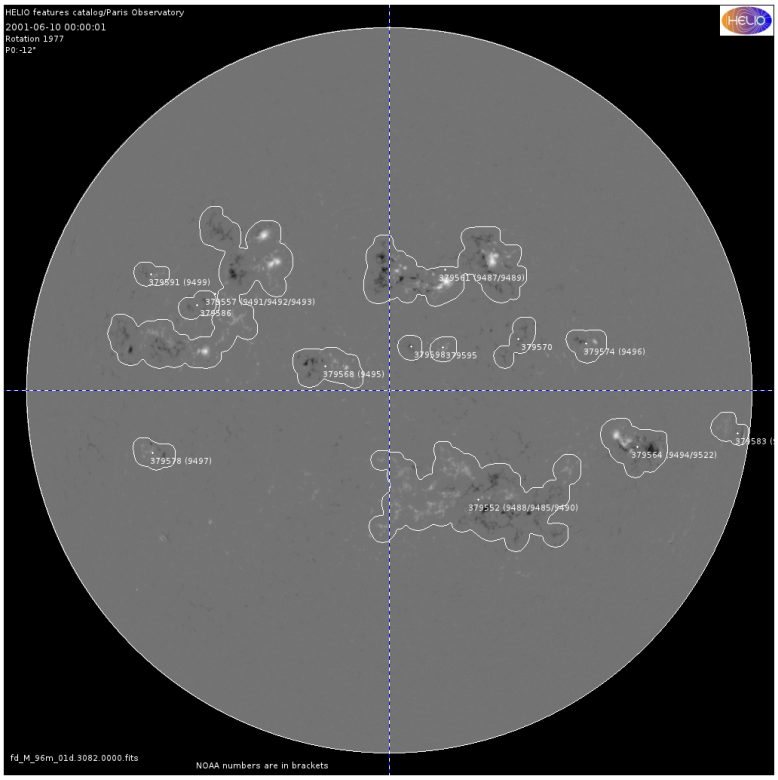

Fig. 1. Magnetogram of the Sun observed on June 10, 2001 at 00:00:01 (UTC) by SOHO/MDI. The strength of line-of-sight magnetic field is represented using gray-scale colors (i.e., white pixels correspond to upward magnetic flux, and dark pixels to downward flux. The contours of detected ARs are indicated by the white lines, and the corresponding gravity centers by white dots. When it is possible, the NOAA region numbers associated with ARs are given in brackets.

2.2 Coronal Holes

The coronal holes (CHs) detection tool applied in HELIO is the *Coronal Hole Automated Recognition and Monitoring* algorithm (CHARM) (Krista & Gallagher 2009). CHARM uses SOHO/EIT (Delaboudinière et al. 1995) 195 ÀĮL and SOHO/MDI line-of-sight magnetograms to detect CHs and has the ability to provide real-time high-speed solar wind forecasts at Earth and compare the predictions with *in-situ* solar wind data. The technique used is based on local intensity thresholding. Each EIT image is partitioned and the local intensity

minimum between the quiet Sun and the low intensity regions is extracted. The low intensity regions are distinguished from other regions based on the magnetic field information obtained from SOHO/MDI magnetograms. Figure 2 illustrates the detection of CHs on a Lambert projection representation of a SOHO/EIT 195 AÌŁ image of the Sun, observed on January 13, 2008 at 10:00:00 (UTC). The light intensity (represented by green scale) is showed as a function of the heliographic longitude and latitude (in degrees). Contours of the detected CHs are indicated by white lines.

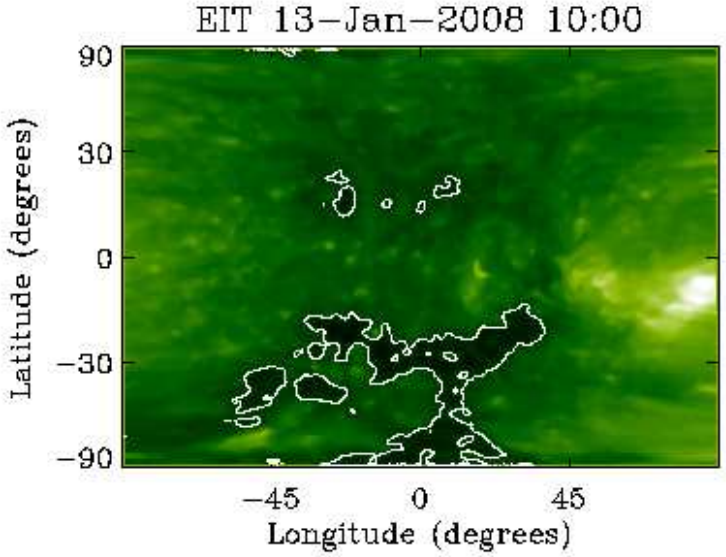

Fig. 2. Lambert projection representation of a SOHO/EIT 195 AÌŁ image of the Sun, observed on January 13, 2008 at 10:00:00 (UTC). The light intensity (represented by green scale) is showed as a function of the heliographic longitude and latitude (in degrees). Contours of the detected CHs are indicated by white lines. (Courtesy of L.Krista.)

2.3 Solar filaments

Detection of solar filaments on Halpha images used in HELIO, was previously developed in the frame of the European Grid for Solar Observations (EGSO) FP5 project. It has been successfully applied on Meudon spectroheliograph observations in order to populate HFC. A description of the method can be found in Fuller et al. (2005). To extract filaments parameters, several cleaning processes are first run in order to correct images from defects characteristic of the instrument (which may lead to spurious detections). Then, filament areas are segmented using a region growing method based on local pixels statistics thresholdings. From segmented filaments, a morphological closing operator is applied to merge close regions that could be considered as a single feature. Finally, skeletons of detected filaments are defined using thinning followed by pruned methods (Gonzalez & Woods 2002). Figure 3 presents results of extracted filaments on a Meudon Halpha spectroheliogram.

Automatic tracking of solar filaments has been also developed in order to identify co-rotating features on successive images (bonnin et al., submitted). The algorithms is based on a curve matching method that allows comparison between filaments skeletons, these latter being previously extracted from several successive images by the dedicated recognition code. In order to counterbalance the solar rotation effects, the matching algorithm is applied on a reference frame which rotates with the solar surface at the Carrington speed (i.e., $v \sim 360/27.2753$ *degrees/day*). On such a reference frame, extracted skeletons of a single co-rotating feature from successive images, will be located at the same coordinates position. A level-of-trust parameter is then computed from each comparison, that will allow to determinate if the tracking is reliable or not. If it is, an unique tracking identification number is allocated to the co-rotating filament on each image. This number will permit, among others, to report in a last step, the filament behaviours (e.g, disappearance before the West limb, *disparitions brusques*, etc.).

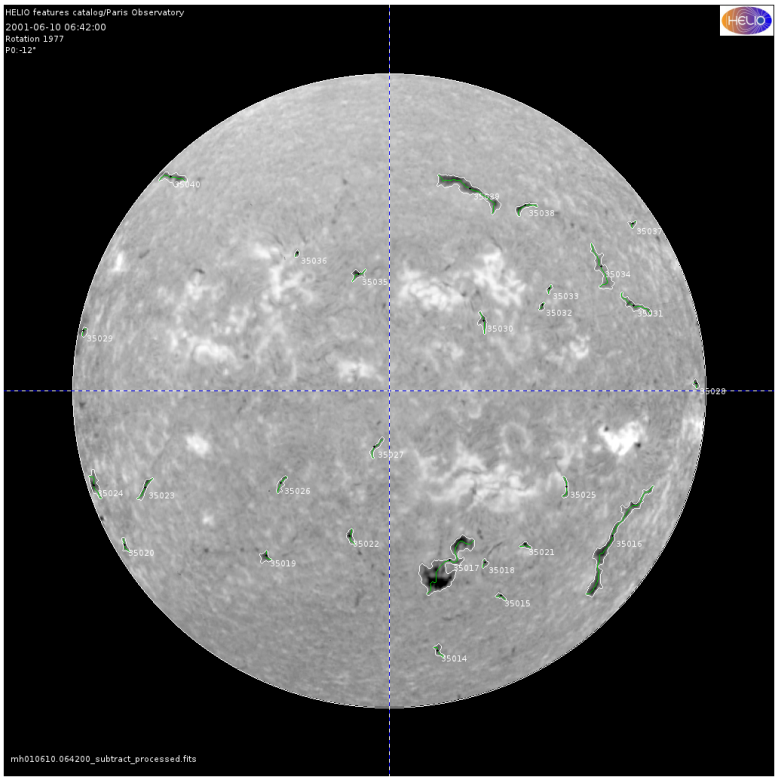

Fig. 3. Halpha image of the Sun observed by the Meudon spectroheliograph on June 6, 2001 at 06:42:00 (UTC). Intensity of light is represented by gray scale colors. Boundaries lines of detected filaments are over-plotted in white, and skeleton lines in green. (This image was produced using the HFC interface.)

3 Recognition of Heliospheric features

3.1 Type III Solar Radio Bursts

In the frame of HELIO, type III solar radio bursts automated recognition is performed by the *RAdio Bursts Automated Tracking* (RABAT) algorithm. This algorithm is based on a technique developed by Lobzin et al. (2009) for the coronal type III bursts detection. Although this latter was initially tested on ground based observatories, covering the approximately 10 to 100 MHz frequency range, it can also be successfully applied with minor corrections on space based observatories, for bursts observed below approximately 10 MHz. Hence, from a modified version of the algorithm, daily dynamical spectra produced by Wind/Waves radio experiment (Bougeret et al. 1995) between 1995 and 2011 has been processed. Detection of type III bursts has been realized separately on the $[\sim 0.01, 1\ MHz]$ and $[\sim 1, 10\ MHz]$ frequency ranges, corresponding respectively to the RAD1 and RAD2 receivers spectral domains, and using a average time resolution of 60 seconds.

The first processing steps of the tracking technique is quite similar to the ones used by Lobzin et al. (2009), and consists to clean the dynamical spectrum (which can be seen as a 2 dimensions image giving the radio intensity as a function of time and frequency) in order to remove radio interference frequencies (RFI), or time periods of instrument calibration. Interpolated values are allocated to these "bad" pixels, which will be not saved in the final event extraction process. A smoothing filter is also applied to improve signal on noise ratio of the image, and a $1/f$ representation of the dynamical spectrum is used, where type III emissions almost appears as straight lines (since the drifting rate df/dt is proportional to $\sim -0.01 f^2$), as illustrated in the left panel of Figure 4.
Then, a binary mask of the cleaned dynamical spectrum is generated, by setting its pixels value to 1 for all the local maxima along time axis at each frequency (all others pixels values are null). On this mask, a type III burst forms a straight line of maxima surrounded by null pixels, as seen in the right panel of Figure 4. These maxima and null pixels correspond respectively to the burst maximal intensities and to the growth and decay

phases, which are drifting with frequency. Using a specific Hough transform and a suitable threshold value, type III bursts main directions can be thus deduced from the binary mask. As HFC stores intensity, location as well morphological information of detected features, a last step is dedicated to extract bursts contours from the dynamical spectrum. These contours are defined by searching the onset and offset times of detected events at each frequency (to filter bad points, fitting processes are applied on onset/offset times versus frequency curves). Finally, as for the others HFC features, bursts boundaries are described using a chain code method.

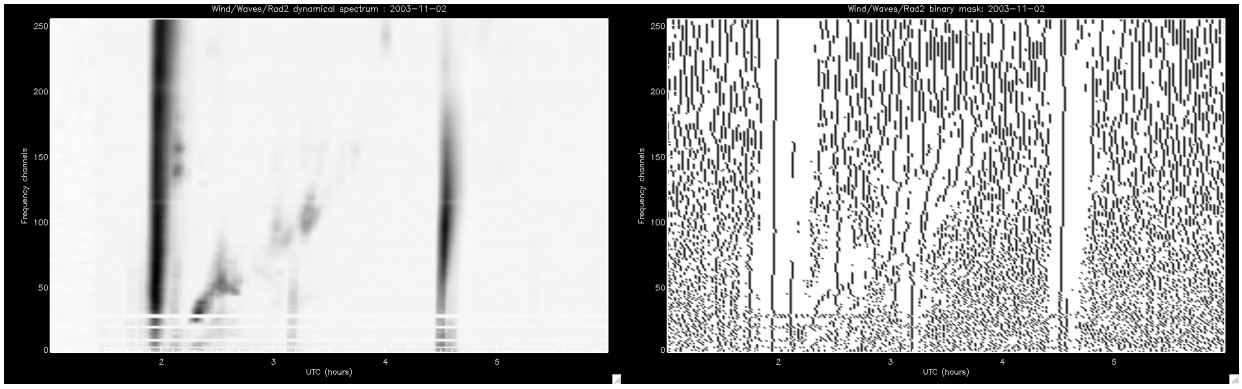

Fig. 4. Left: Zoom on a pre-processed dynamical spectrum of the Wind/Waves Rad2 receiver for the November 2, 2011. The radio flux is showed in gray scale as a function of time and frequency channels ($1/f$ representation). Two type III bursts, which appear as intense (i.e., darker) fast drifting emissions can be seen at about 01:55 and 04:30 respectively (a type II burst, which starts at the same time than the first type III is also visible).**Right:** Corresponding binary mask portion. Type III events can be distinguished from noise by long vertical lines of local maxima, surrounded by null pixels.

4 Future works

We presented here an overview of HELIO/HFC efforts in terms of automated recognition and tracking capabilities. Since the HELIO project is still in progress, this description must be seen as a snapshot of the current development status, which will strongly evolved with the addition of new features data in HFC. Especially, active regions detection will be extended to others available observations and at several wavelengths (e.g. SOHO/EIT and STEREO/EUVI). Sunspots detection (not described here) will be systematically applied on SOHO/MDI as well as SDO/HMI intensity images. Solar filaments algorithm has been successfully tested on Big Bear Solar Observatory (BBSO) data, and should be implemented in the next few months. As previously mentioned, prominences data will be also accessible from HFC. Type III as well as type II bursts detections will be extended to STEREO/Waves and Nançay Decametric Array dataset. Tracking information will be also provided for several features (the SMART algorithm already offers tracking capabilities that will be run in HELIO). Beyond the HFC needs, relevant information, extracted from all these codes, will be used by the HELIO system to provide efficient propagation tools to users, allowing time and space associations between events and features observed on the heliosphere.

HELIO is a Research Infrastructures funded under the Capacities Specific Programme within the European Commission's Seventh Framework Programme (FP7; Project No. 238969).

References

Bougeret, J.-L., Kaiser, M. L., Kellogg, P. J., et al. 1995, Space Sci. Rev., 71, 231
Delaboudinière, J.-P., Artzner, G. E., Brunaud, J., et al. 1995, Sol. Phys., 162, 291
Fuller, N., Aboudarham, J., & Bentley, R. D. 2005, Sol. Phys., 227, 61
Gonzalez, R. C. & Woods, R. E. 2002, Digital image processing, ed. Gonzalez, R. C. & Woods, R. E.
Higgins, P. A., Gallagher, P. T., McAteer, R. T. J., & Bloomfield, D. S. 2011, Advances in Space Research, 47, 2105
Krista, L. D. & Gallagher, P. T. 2009, Sol. Phys., 256, 87
Lobzin, V. V., Cairns, I. H., Robinson, P. A., Steward, G., & Patterson, G. 2009, Space Weather, 70, S04002
Scherrer, P. H., Bogart, R. S., Bush, R. I., et al. 1995, Sol. Phys., 162, 129